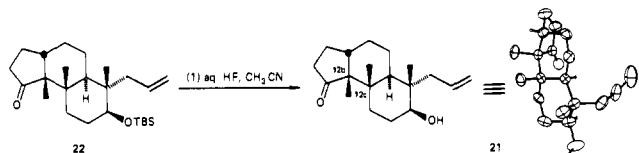


followed by methanolysis (MeOH, H₂SO₄). Triols **20a,b** (6:1) were then subjected to a 1:1 mixture (v/v) of H₂SO₄(conc)-MeOH (0 °C, 20 min) to afford enone **16** [$[\alpha]^{25}_D + 46^\circ$ (*c* 1.6, CHCl₃)]¹¹ in modest but useful yield.¹⁶

With enone **16** in hand, we turned to the reductive alkylation sequence, the cornerstone of our synthetic strategy. Toward this end, enone **16** protected as the *tert*-butyldimethylsilyl ether (TBSCl, imidazole, DMAP, DMF, 95%) was dissolved in THF containing 0.9 equiv of H₂O and added to a lithium-ammonia solution (0.25 M) held at -78 °C.¹⁷ Alkylation of the derived lithium enolate at -78 °C with MeI afforded a single product in 50% yield. To our surprise, single-crystal X-ray analysis of alcohol **21**,¹¹ derived from **22**¹¹ by deprotection (aqueous, HF, CH₃CN;



mp 113.5–114.5 °C), indicated that the crucial reductive alkylation had afforded **22** in which the C(12b), C(12c) vicinal methyl groups were disposed *cis*, not *trans* as required for paspaline (**1**). Fortunately for the paspaline synthetic venture, modification of the reductive alkylation process, in particular execution of the alkylation under conditions that more closely resembled those of Trost (i.e., inverse addition of the enolate to a solution of MeI-HMPA held at +50 °C) led in 50% yield to a 2:1 mixture of **22** and **15**,¹¹ respectively, in addition to a small amount (10–15%) of unalkylated material. All attempts to enhance further the ratio of **15** relative to **22** proved unsuccessful. Separation was achieved via flash chromatography¹⁴ after selective reduction (NaBH₄, CH₃OH, 0 °C) of the unalkylated material.

Our attention next focused on annulation of the pyranyl ring system. First, a two-carbon chain extension led to olefins **26** (*Z:E* = 85:15);¹¹ the overall yield of this four-step sequence was 54%. Ring formation was then accomplished via treatment of **26** with an unbuffered solution of MCPBA in CH₂Cl₂ to afford a mixture of pyranyl alcohols **27**. Without separation the latter were oxidized (PCC, CH₂Cl₂, 4 Å molecular sieves)¹⁸ and equilibrated (K₂CO₃, MeOH) to provide diketones **28a** and **28b** (85:15, respectively)¹¹ in 81% yield. Recrystallization (hexane-ether) improved this ratio to 95:5. Finally, introduction of the methyl group (MeMgCl, THF) proceeded without event to afford **14** (80%, mp 149–150.5 °C).¹¹ The chemoselectivity observed here is attributed to the steric encumbrance of the cyclopentyl carbonyl group.

With construction of the diterpenoid portion of paspaline complete, there remained only introduction of the indole nucleus. We selected the Gassman procedure.¹⁹ Treatment of **14** with LDA [3 equiv, THF-HMPA (1:1)] followed by addition of dimethyl disulfide (4 equiv) led to 1:1 mixture of thiomethyl ketones (**29a,b**,^{11,20} 92%), shown by NMR (250 MHz) to be epimeric only at C(7a). Reaction of the latter with *N*-chloroaniline (aniline, CH₂Cl₂, *tert*-butyl hypochlorite, -78 °C) followed by addition of triethylamine and reduction with Raney Ni (EtOH) resulted in efficient [2,3]-sigmatropic rearrangement, rearomatization, and reductive removal of the thiomethyl substituent to provide **30** [$[\alpha]^{24}_D + 122^\circ$ (*c* 0.5, CHCl₃)]¹¹ as a single compound (250-MHz

NMR). It is interesting to note that **30** and its immediate precursor preferred to exist in the ketoaniline form rather than undergo spontaneous dehydration. Dehydration (PTSA, CH₂Cl₂, Δ), however, proved straightforward to afford (-)-paspaline (**1**) [$[\alpha]^{24}_D - 42^\circ$ (*c* 0.6, benzene); natural paspaline $[\alpha]^{24}_D - 38.5^\circ$ (*c* 0.47, benzene)]²¹ in 83% yield. That in fact (-)-paspaline was in hand derived from careful comparison of the physical and spectral properties with those of an authentic sample kindly provided by Professor Arigoni.²²

In summary, the first total synthesis of (-)-paspaline (**1**) has been achieved. The synthesis proceeded in 23 steps from Wieland-Miescher ketone, afforded (-)-paspaline in high enantiomeric purity, and for the most part was highly stereocontrolled.

Acknowledgment. It is a pleasure to acknowledge the support of this investigation by the National Institutes of Health (Institute of Neurology and Communication Disorders and Stroke) through Grant 18254. In addition, we thank Drs. George Furst and Patrick Carroll of the University of Pennsylvania Spectroscopic Facilities for aid in obtaining the high-field NMR and X-ray spectral data, respectively.

(21) Reference 2a reports a rotation of $[\alpha]_D - 23^\circ$ (*c* 0.36, chloroform).

(22) We thank Professor D. Arigoni of the Eidgenössische Technische Hochschule Zürich, for providing a very generous sample of (-)-paspaline (**1**) as well as for copies of the spectra.

Structure of a Heteropoly Blue. The Four-Electron Reduced β-12-Molybdophosphate Anion

Julie N. Barrows, Geoffrey B. Jameson,* and Michael T. Pope*

Department of Chemistry, Georgetown University
Washington, DC 20057

Received November 26, 1984

Despite wide analytical applications involving "molybdenum blues"¹ and current interest in mixed-valence chemistry,² definitive evidence concerning the electronic and molecular structures of heteropoly blues³ is scarce. Contributions from the Université Pierre et Marie in Paris and from our laboratory have established, via ESR, that one-electron reduced heteropolymolybdates and -tungstates are class II mixed-valence species with weakly trapped (thermally mobile) Mo⁵⁺ or W⁵⁺ centers.⁴ More highly reduced heteropolyanions are ESR silent and the extent or nature of the delocalization is unclear.⁵

Fruchart and Souchay have shown that reduction of the Keggin-structure anion α-[PMo₁₂O₄₀]³⁻ leads, in aqueous acidic solutions, to stable heteropoly blues derived from an isomeric (β) anion.⁶ It has generally been assumed⁷ that the β-12-molybdates

(1) See, for example: Murphy, J.; Riley, J. P. *Anal. Chim. Acta* **1962**, *27*, 31.

(2) Brown, D. B., Ed. "Mixed Valence Compounds"; Reidel: Dordrecht, 1980. Day, P. *Int. Rev. Phys. Chem.* **1981**, *1*, 149.

(3) Pope, M. T. "Heteropoly and Isopoly Oxometalates"; Springer-Verlag: New York, 1983; Chapter 6.

(4) (a) Prados, R. A.; Pope, M. T. *Inorg. Chem.* **1976**, *15*, 2547. (b) Launay, J. P.; Fournier, M.; Sanchez, C.; Livage, J.; Pope, M. T. *Inorg. Nucl. Chem. Lett.* **1980**, *16*, 257. (c) Che, M.; Fournier, M.; Launay, J. P. *J. Chem. Phys.* **1979**, *71*, 1954. (d) Sanchez, C.; Livage, J.; Launay, J. P.; Fournier, M.; Jeannin, Y. *J. Am. Chem. Soc.* **1982**, *104*, 3194. (e) Sanchez, C.; Livage, J.; Doppelt, P.; Chauveaux, F.; Lefebvre, J. *J. Chem. Soc., Dalton Trans.* **1982**, 2439.

(5) It has, however, been inferred from ¹⁷O NMR that the extra electrons in the two-electron blue of [P₂Mo₁₈O₆₂]⁶⁻ are localized on Mo atoms in the two equatorial belts of the Dawson structure (Kazansky, L. P.; Fedotov, M. A. *J. Chem. Soc., Chem. Commun.* **1980**, 644).

(6) Fruchart, J. M.; Souchay, P. *C. R. Hebd. Seances Acad. Sci., Ser. C* **1968**, *266*, 1571. This anion (λ_{max} 830 nm; ε ca. 28 000 M⁻¹ cm⁻¹) appears to be the complex formed in a widely used "molybdenum blue" spectrophotometric determination of phosphorus.¹

(7) Thouvenot, R.; Fournier, M.; Franck, R.; Rocchiccioli-Deltcheff, C. *Inorg. Chem.* **1984**, *23*, 598.

(15) (a) Islam, A. M.; Raphael, R. A. *J. Chem. Soc.* **1953**, 2247. (b) Baumann, M.; Hoffman, W.; Muller, N. *Tetrahedron Lett.* **1976**, 3585. (c) Hiyama, T.; Shinoda, M.; Saimoto, H.; Nozaki, H. *Bull. Chem. Soc. Jpn.* **1981**, *54*, 2747. (d) MacAlpine, G. A.; Raphael, R. A.; Shaw, A.; Taylor, A. W.; Wild, H.-J. *J. Chem. Soc., Perkin Trans. 1* **1976**, 410.

(16) Several minor products were also isolated. Structural identification of these products will be reported in our full account of this work.

(17) For best results, the concentration of the lithium-ammonia solution should be 0.25 M or greater, in order that the radical anion can compete effectively for the limited amount of water.

(18) Herscovici, J.; Egron, M.-J.; Antonakis, K. *J. Chem. Soc., Perkin Trans. 1* **1982**, 1962.

(19) Gassman, P. G.; van Bergen, T. J.; Gilbert, D. P.; Cue, B. W., Jr. *J. Am. Chem. Soc.* **1974**, *96*, 5495 and references therein.

(20) Trost, B. M.; Salzmann, T. N.; Hiroi, K. *J. Am. Chem. Soc.* **1976**, *98*, 4887.

Table I. Selected Metrical Details of Keggin Anions Averaged to $\bar{3}$ Symmetry^a

anion	(M _a ...M _a)(M _a ...M _b)		M _b ...M _b		(M _c ...M _c)(M _c ...M _c)		symm imposed	ref
	3 edge	6 corner	3 edge	3 corner	6 edge	3 corner		
α -PW ₁₂ O ₄₀ ³⁻	3.41	3.70					$\bar{4}3m$	10
α -PMo ₁₂ O ₄₀ ³⁻	3.41	3.71		pseudo-23	symmetry		1	11a
α -SiMo ₁₂ O ₄₀ ⁴⁻	3.36	3.70		pseudo-23	symmetry		1	11b
β -SiW ₁₂ O ₄₀ ⁴⁻	3.34	3.66	3.32	3.71	3.36	3.71	<i>m</i>	8a
β -SiW ₁₂ O ₄₀ ⁴⁻	3.35	3.65	3.31	3.74	3.37	3.68	1	8b
β_1 -SiMoW ₁₁ O ₄₀ ⁴⁻	3.35	3.65	3.32	3.73	3.36	3.70	<i>m</i>	8c
β -PMo ₁₂ O ₄₀ ⁷⁻	3.49	3.65	3.56	3.67	3.41	3.77	3	

^a With respect to the unique 3-fold axis of the β -Keggin anion, the Mo atoms of the rotated Mo₃ triad of edge-shared octahedra are denoted Mo_a; the Mo atoms of the alternately edge- and corner-shared ring of 6Mo octahedra are denoted Mo_b; the Mo atoms linked by edges to Mo_b and by corners to each other are denoted Mo_c.

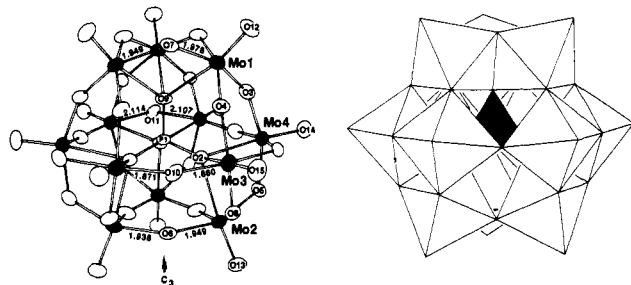


Figure 1. Diagram showing atom labeling and selected metrical details for [H₂PMo₁₂O₄₀]⁷⁻ alongside a polyhedral representation of the anion. Boundary ellipsoids in the former are drawn at the 50% probability level. Estimated standard deviations are ± 0.008 Å.

are isostructural with β -[SiW₁₂O₄₀]⁴⁻,⁸ although this has never been proved. We report here the crystal structure of Ca_{0.5}H₆PMo₁₂O₄₀·ca. 18H₂O isolated from a solution of the four-electron blue of the β -series (" β -IV").⁹

(8) (a) Fuchs, J.; Thiele, A.; Palm, R. *Z. Naturforsch., B: Anorg. Chem., Org. Chem.* **1981**, *36B*, 161. (b) Matsumoto, K. Y.; Kobayashi, A.; Sasaki, Y. *Bull. Chem. Soc. Jpn.* **1975**, *48*, 3146. (c) Robert, F.; Tézé, A.; Hervé, G.; Jeannin, Y. *Acta Crystallogr., Sect. B* **1980**, *B36*, 11.

(9) Crystals were grown by slow cooling of a concentrated aqueous solution containing the heteropoly blue acid β -H₂PMo₁₂O₄₀ (Rocchiccioli-Delcheff, C.; Fournier, M.; Franck, R.; Thouvenot, R. *Inorg. Chem.* **1983**, *22*, 207) to which CaCl₂·2H₂O was added. Most crystals showed trigonal symmetry $\bar{3}$ with absences consistent with the space groups *P31c* or *P31c* and unit cell dimensions $a = b = 13.77$ Å and $c = 31.75$ Å and diffracted poorly with high thermally diffuse scattering. One crystal, which diffracted well, showed trigonal $\bar{3}$ symmetry and systematic absences $-h + k + l = 3n$ and $h - k + l = 3n$, corresponding to a rhombohedral crystal twinned about 1100 in the *R*-centered hexagonal setting. Following data collection the crystal was analyzed by electron microprobe analysis with the following results: CaO:MoO₃:P₂O₅ = 1.00:23.98:1.02. The crystal was subsequently dissolved in 0.1 M HCl and gave an absorption spectrum (λ_{\max} 830 nm) identical with that produced by a solution of the bulk material. Crystal data: space group *R* $\bar{3}$, $a = b = 13.798$ (3) Å, $c = 41.511$ (9) Å (using 26 reflections in the range 0.4004 < (sin θ)/ λ < 0.4357 Å⁻¹ avoiding reflections for which $h - k + l = 3n$ and $-h + k + 3l = 3n$); $Z = 6$, 3-fold symmetry imposed on the [PMo₁₂O₄₀]⁷⁻ anion. Data collection: Picker FACS-I automatic diffractometer with on-line profile analysis (NRC-Canada); Mo K α graphite-monochromated radiation; 5828 data with (sin θ)/ λ < 0.5946 Å⁻¹, after an empirical absorption correction (correction factors 0.76–1.00), averaging ($R_{av} = 0.028$ on F^2), and elimination of reflections $h - k + l = 3n$ and $-h + k + 3l = 3n$ left 1632 data of which the 1191 data with $F_o^2 > 3\sigma(F_o^2)$ and (sin θ)/ $\lambda > 0.12$ Å⁻¹ were used in full-matrix least-squares refinements. The structure was solved by MULTAN84 of the Enraf-Nonius SDP, retaining for this calculation the data for which $l = 3m$ and taking $F_{hk3m} = F_{hk3m}/2^{1/2}$. Current values for R and R_w on F are 0.043 and 0.058 for a model in which all nonhydrogen atoms are granted anisotropic thermal parameters. The weighting scheme is $w = 1/\sigma^2$ where $\sigma^2 = \sigma_{counting}^2 + (0.05F_o^2)^2$. Residual electron density is concentrated near Mo1, but the maximum peak density is only 0.80 e/Å³. Parallel refinements using data from the other twin lead to essentially identical parameters, with differences between the two structures not exceeding twice the esd of the difference. With the final parameters from these refinements, structure factors were calculated for those data suffering overlap ($l = 3n$). When F_{hkl}^2 and $F_{\bar{h}\bar{k}l}^2$ are appropriately scaled and combined, the values for R and R_w on F^2 for the $l = 3n$ data are 0.058 and 0.070. It is not expected that future refinements upon F^2 , using a modified least-squares program to calculate F_{hkl}^2 , where $F_{hkl}^2 = \chi F_{hkl}^2 + (1 - \chi)F_{\bar{h}\bar{k}l}^2$ and χ is a variable parameter for the relative twin volumes, will lead to any significant changes in the structure of the anion, although markedly decreased estimated standard deviations are to be expected. Tables of atomic parameters and structure factor amplitudes have been deposited as supplementary material.

The reduced [PMo₁₂O₄₀]⁷⁻ anion, illustrated in Figure 1, has indeed the same overall structure observed for β -[SiW₁₂O₄₀]⁴⁻ and β_1 -[SiMoW₁₁O₄₀]⁴⁻ anions but with some significant dimensional differences. Since the substitution of Mo for W and Si for P has little effect on the M...M separations in α -Keggin anions (Table I^{8,10,11}) we may confidently describe the perturbations wrought on the β -structure by reduction. The major effect is a symmetrical expansion of the metal atom framework away from the anion's 3-fold axis. As shown in Table I, the Mo...Mo separations among edge-shared octahedra of the rotated triad (Mo_a) and of the adjacent central belt (Mo_b) are substantially lengthened, while the Mo separations among the corner-shared Mo_b octahedra are significantly shortened. The average Mo...Mo separation in the central belt suffers a net increase of 0.12 Å. The corner-shared Mo...Mo separations in the lower triad of Figure 1 are also greater than in the oxidized α -structures, but we note that the remaining Mo...Mo separations (between the belt and the upper and lower triads) are quite normal. The Mo–O bond lengths fall in the ranges commonly observed except for those involving the oxygen atoms (O11) at the edge-shared contacts in the central belt, for which Mo–O is 2.110 (8) Å (cf. 1.92 Å for the oxidized structures) and Mo–O–Mo is 114.9 (3)° (cf. 92° for the oxidized structures). We conclude that these three oxygen atoms are protonated.¹²

The question arises as to the location of the four additional electrons. The polyanion has crystallographically imposed 3-fold symmetry and the deviations from 3*m* (*C*_{3v}) symmetry are mostly statistically insignificant. The modest thermal parameters of the Mo atoms ($B_{\text{equiv}} < 2.24$ (3) Å² and root-mean-square components of thermal displacements in the range 0.13–0.19 Å) and of the P and O atoms ($B_{\text{equiv}} < 3.1$ (3) Å²) indicate an absence of dynamic or static disorder.¹³ We may therefore conclude that the four electrons occupy delocalized molecular orbitals. Although the reduced difference in Mo...Mo separations between edge- and corner-shared octahedra of the central belt is consistent with a delocalized arrangement of the added electrons in the belt, it is not possible to determine whether the expansion of the rotated triad is due to the presence of an electron(s) or is a consequence of the expansion of the central belt. Theoretical and spectroscopic investigations are in progress.

Acknowledgment. We thank E. Jarosewich, J. A. Nelen, and P. J. Dunn of the Department of Mineral Sciences, Smithsonian

(10) Brown, G. M.; Noe-Spirlet, M.-R.; Busing, W. R.; Levy, H. A. *Acta Crystallogr., Sect. B* **1977**, *B33*, 1038.

(11) (a) D'Amour, H.; Allmann, R. Z. *Kristallogr., Kristallgeom., Kristallphys., Kristallchem.* **1976**, *143*, 1. (b) Feist, M.; Molchanov, V. N.; Kazanskii, L. P.; Torchenkova, E. A.; Spitsyn, V. I. *Russ. J. Inorg. Chem. (Engl. Transl.)* **1980**, *25*, 401.

(12) Such a bond length involving bridging OH is precedented: W–OH(W) = 2.15 Å in [(C₆H₅AsO₃)₂W₆O₁₈(OH)]³⁻ (Wasfi, S. H.; Kwak, W.; Pope, M. T.; Barkigia, K. M.; Butcher, R. J.; Quicksall, C. O. *J. Am. Chem. Soc.* **1978**, *100*, 7786). The complex studied here was crystallized as the hemicalcium salt with the calcium located with half occupancy on the 3-fold axis near the $\bar{3}$ site. The tetrahedrally coordinated calcium is disordered about the inversion center as a consequence. Six protons are required for charge balance. On the basis of the observed variation of the half-wave potentials with pH,⁵ the heteropoly blue anion should be tetraprotonated at least. Given the location of three protons on the O11 atoms, the remaining proton(s) are presumed to be disordered over other bridging oxygen sites.

(13) For a discussion of crystallographic disorder in heteropoly structures, see: Evans, H. T., Jr.; Pope, M. T. *Inorg. Chem.* **1984**, *23*, 501.

Institution, for electron microprobe analysis. G.B.J. gratefully acknowledges the support of the Research Corporation and the NIH-BRSG for the renovation of X-ray diffraction facilities and the purchase of graphics equipment. M.T.P. acknowledges support of NSF through Grant CHE8306736.

Supplementary Material Available: Tables giving final atomic parameters, anisotropic thermal parameters, structure factor amplitudes, and selected interatomic distances and angles (13 pages). Ordering information is given on any current masthead page.

Effect of Semiconductor on Photocatalytic Decomposition of Lactic Acid

H. Harada,*† T. Sakata,† and T. Ueda†

*Meisei University, Department of Chemistry
Faculty of Science and Engineering
Hino-shi, Tokyo 191
Institute for Molecular Science
Myodaiji, Okazaki 444, Japan*

Received July 13, 1984

Revised Manuscript Received January 7, 1985

Photocatalytic reactions of particulate semiconductors have been investigated not only from the viewpoint of solar energy conversion but also from that of organic synthesis. From this viewpoint, the specificity of the photocatalyst to a given reaction is important to control the reaction. Here we report the dependence of the photocatalytic reaction of lactic acid on the kind of semiconductor. Platinized TiO₂ and CdS were found to decompose lactic acid very efficiently. The quantum yield of hydrogen production amounts to 71% (at 360 nm) for Pt/TiO₂ and 38% (at 440 nm) for Pt/CdS. Interestingly, a clear difference was observed in the reaction products, depending on the kind of semiconductor. For Pt/TiO₂, the main products are H₂, CO₂, and acetaldehyde, whereas for Pt/CdS they are H₂ and pyruvic acid. Photocorrosion of CdS was found to be suppressed during the reaction and the photocatalytic activity was maintained for more than 300 h of irradiation.

As powdered semiconductors, cadmium sulfide (Katayama Kagaku Co., cubic and average size 0.6 μm) and titanium dioxide (Furuuchi Chem. Co., rutile, and average size 0.5 μm) were used. Platinized TiO₂ (Pt/TiO₂) was prepared by depositing Pt photochemically on the surface of TiO₂.¹ Pt/CdS was prepared by mixing CdS with 5% Pt black.² Each photocatalyst was suspended in a lactic acid-water mixture (1:10 in volume) and irradiated after evacuation with a 1-kW Xe lamp (under 500-W operation). After irradiation the gaseous reaction products were trapped and analyzed by a quadrupole mass spectrometer (Anelva, AGA-360) as described previously.² The yield of gaseous products was determined from the pressure measured by a pressure gauge (Datametrics). The liquid reaction products were analyzed by a steam carrier gas chromatograph (Ohkura Denki, Model 103) and a liquid chromatograph (Shimadzu, LC-4A).

In each case, when the glass bulb containing the photocatalyst suspended in the lactic acid solution was irradiated with white light from the Xe lamp, gas bubbles evolved vigorously. The gaseous products were H₂ and CO₂ for Pt/TiO₂ and only H₂ for Pt/CdS. The quantum yields of H₂ production are quite high as shown in Table I. The wavelength dependence of the quantum yield indicated that the band-gap excitation of the semiconductor is essential to the reaction. Since a clear difference was observed in the gaseous products for Pt/TiO₂ and Pt/CdS, the reaction

Table I. Quantum Yields for H₂ Production from Lactic Acid-Water (1:1 vol) Solution^a

cat.	wavelength/nm	quantum yield
Pt/TiO ₂	420	0.03
	400	0.43
	380	0.64
	360	0.71
Pt/CdS	520	0.08
	500	0.12
	480	0.21
	460	0.26
	440	0.38

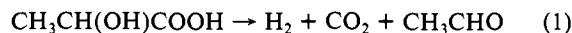
^aQuantum yields were based on incident photon flux, which was measured by a thermopile (Eppley Lab. Inc.).

Table II. Photocatalytic Reaction Products from Lactic Acid-Water (1:10 vol) Solution^a

cat. ^b	prod./mmol					
	H ₂	CO ₂	CH ₃ CHO	C ₂ H ₅ OH	CH ₃ -COOH	CH ₃ -COCOOH
Pt/TiO ₂	1.21	1.43	1.08	0.047	0.151	0.02
Pt/CdS	1.20	0.015				0.80

^aIrradiated with 1-kW Xe lamp (under 500-W operation) for 4 h. ^b300 mg of catalyst was used. In the case of Pt/CdS, the photocatalyst prepared by photochemical deposition of Pt showed a poorer activity than the photocatalyst by mechanical mixing. Therefore, in the present experiment the photocatalyst prepared by the latter method was used. There was no dependence of the distribution of the reaction products on the preparation method.

products in aqueous medium were also analyzed. Table II shows the results after 4 h of irradiation. Since a large excess of lactic acid, about 30 mmol, was used as the reactant, the result in this table should be considered as for an initial stage of the reaction. As shown in this table, for Pt/TiO₂, the amounts of H₂, CO₂, and CH₃CHO are nearly equal. This result suggests that the following reaction takes place:



Ethanol, acetic acid and pyruvic acid were produced as minor products. The production of ethanol and acetic acid can be explained by decarboxylation of lactic acid and the oxidation of acetaldehyde in water, respectively.³ On the other hand, for Pt/CdS, the main products are hydrogen and pyruvic acid. Only a trace amount of CO₂ was produced and no acetaldehyde was detected, which is in strong contrast with the case of Pt/TiO₂. Since the products were quite different from that for Pt/TiO₂, we cannot apply reaction 1 to this system. The following reaction is proposed for Pt/CdS:



The ratio of the yield of H₂ to that of pyruvic acid is a little larger than the ratio (1.0) expected from reaction 2. Liquid chromatography indicates that some unidentified compounds are produced as minor products together with pyruvic acid, which might explain the above discrepancy. The decomposition of pyruvic acid produced from reaction 2 can be discounted because of the small yield of CO₂.⁴

The anodic current due to the oxidation of lactic acid begins to rise at about 1.1 V vs. SCE at a glassy carbon electrode in 0.5 M K₂SO₄ solution. Since the valence band edge of CdS is located at 1.6 V vs. SCE,⁵ lactic acid can be oxidized with CdS as well as TiO₂. A clear difference in the reaction can be explained by the difference in oxidation power of the hole in the valence band. It is known that ethanol can be decomposed efficiently with both of these two semiconductor photocatalysts. However, acetic acid is decomposed with TiO₂ but not with CdS,⁶ because the oxidation

* Meisei University.

† Institute for Molecular Science.

(1) Kraeutler, G.; Bard, A. J. *J. Am. Chem. Soc.* **1978**, *100*, 2239.

(2) Kawai, T.; Sakata, T. *J. Chem. Soc., Chem. Commun.* **1980**, 647.

(3) Sakata, T.; Kawai, T. *Chem. Phys. Lett.* **1981**, *80*, 341.

(4) Miyashita, K.; Sakata, T.; Nakamura, K.; Kawai, T.; Sakata, T. *Photochem. Photobiol.* **1984**, *39*, 151.

(5) Williams, R. *J. Vac. Sci. Technol.* **1976**, *13*, 12.